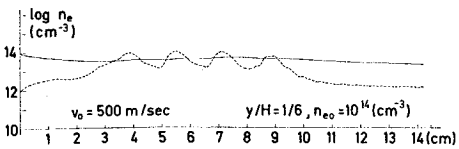

Fig. 3 Electron density distribution at $v_0 = 500$ m/sec and $n_{e0} = 10^{14}$ cm^{-3}.

ture fluctuations, particularly at lower electron densities. The typical relaxation length at this velocity is about 2 cm. The results of computations show that the locus of maximum current density roughly coincides with that of maximum electron density, but is shifted slightly (1–2 mm at the gas velocities considered here) to the side of the maximum electron temperature. Hence, higher electron density on the upstream side of a discharge tends to "pull" the current streamlines forward, thus partially compensating the velocity-sweep. At 100 m/sec gas velocity, the current density distribution remains nearly the same for all three inlet electron density values (the electron densities are approximately the same for $x \gtrsim 3$ cm). The sharp increase of the electron temperature observed in front of the first electrode pair at low inlet electron densities gradually reduces as the inlet electron density increases. This phenomenon, i.e., the necessity for higher electron temperatures at lower electron densities to carry the same current, has been observed experimentally.[6]

The effect of preionization and gas velocity on the performance characteristics of MHD devices can be seen from the data in Table 1. Here the ratio of average to ideal Faraday field strength is given for each electrode pair as function of the preionization level (inlet electron density) and gas velocity. Since the current flow through each electrode pair is kept constant, the ratio $\langle E_y \rangle / E_{y\mathrm{id}}$ is a measure of the "local" (per electrode pair) effective internal resistance of the generator. The quantities appearing in this table arre defined as follows: $\langle E_y \rangle = (1/H)_H \int E_y dy$, $E_{y\mathrm{id}} = \langle v \rangle B + \langle J_y \rangle / \sigma_{\mathrm{id}}$ and σ_{id} is the nonequilibrium conductivity value defined by the average current density under ideal conditions (zero losses, Saha equilibrium, etc.).

As can be seen, at low inlet electron densities the internal resistance increases monotonically with increasing velocity, but only the first few electrode pairs are affected appreciably by the velocity changes. Comparing the cases $v \approx 0$ and $\langle v \rangle = 440$ m/sec ($n_e = 10^{12}$ cm^{-3}), the effective internal resistances differ by a factor of 2.5 at the first electrode pair. At low gas velocities an increase of the inlet electron density has no pronounced effect on the generator performance because the electrons recombine before they reach the first electrode pair. Only when the plasma velocity is high enough and the typical relaxation length exceeds the distance between the preionizer and the first electrode pair does the effect of a high inlet electron density become highly pronounced (compare the case $v_0 = 500$ m/sec, $n_e = 10^{14}$ cm^{-3} with the others in Table 1). This can also be seen by comparing the last electron density distribution of Fig. 2 with Fig. 3: although at $v_0 = 100$ m/sec the electron density first decreases (recombination effect) and then, due to ohmic heat input, increases again in the region of the first electrode pair, at $v_0 = 500$ m/sec it does not succeed in recombining nor in following the electron temperature fluctuations and remains practically constant in the entire active zone of the duct. The corresponding reduction of the effective internal resistance is apparent.

References

[1] Lengyel, L. L., "Computation of Current Distributions in MHD Generators with Allowance for Recombination Effects," *Proceedings of the Eighth Symposium on Engineering Aspects of Magnetohydrodynamics*, Stanford Univ., March 1967, pp. 105–106; also *Energy Conversion*, Vol. 9, 1969, pp. 13–23.

[2] Oliver, D. A. and Mitchner, M., "Nonuniform Electrical Conduction in MHD Channels," *AIAA Journal*, Vol. 5, No. 8, Aug. 1967, pp. 1424–1432.

[3] Lengyel, L. L., "Numerical Simulation of Ionization Instability with Allowance for Dissipative Processes," *Proceedings of the Eleventh Symposium on Engineering Aspects of Magnetohydrodynamics*, California Institute of Technology, March 1970, pp. 193–198.

[4] Cool, A. T. and Zukoski, A. E., "Recombination; Ionization and Nonequilibrium Electrical Conductivity in Seeded Plasmas," *The Physics of Fluids*, Vol. 9, No. 4, April 1966, pp. 780–796.

[5] Kerrebrock, J. L. and Hoffman, M. A., "Nonequilibrium Ionization due to Electron Heating, Pt. II: Experiments," *AIAA Journal*, Vol. 2, No. 6, June 1964, pp. 1080–1087.

[6] Dodel, G., "Experimental Investigaion of Current Density Distributions in an Argon-Potassium Plasma Streaming through a Channel with Segmented Electrodes," *Plasma Physics*, Vol. 12, 1970, pp. 273–292.

Suboptimal Linear Filtering with a Limited State

JOHN R. HATFIELD*
Massachusetts Institute of Technology, Cambridge, Mass.
AND
DONALD ROCKWELL†
Boston University, Boston, Mass.
AND
PAUL ABRAMSON‡
Transportation Systems Center, Cambridge, Mass.

I. Introduction

IN applying Kalman filtering theory to real time filtering problems, it is often found impractical to estimate the complete state every time a measurement is made. In this case, one is forced to settle for some form of suboptimal filtering in which the dimension of the filter state is limited. If the filtering gains are being computed in real time, this problem can sometimes be solved by simplifying the model and perhaps modifying the driving noise and/or the measurement noise to try to compensate in some way for this simplification. The case considered here is the one in which the filtering gains are to be precomputed and stored in the computer. No restriction is placed on the method used to perform these computations, but there is a restriction on the number of gains that can be stored.

If the complete state is not being estimated, and one attempts to find a "best" set of gains to estimate the partial state recursively, the performance of the resulting filter can be very surprising. The purpose of this note is to illustrate some of these difficulties in the context of a simple example problem.

II. Statement of the Problem

Consider an aircraft flying towards a landing site at a known constant velocity. It is desired to estimate the range to go with radar range measurements that contain errors due to an unknown scale factor as well as wideband (white) measurement noise. Although the actual measurements, which can be written as the product of the range and scale factor plus the

Received October 13, 1970; revision received December 28, 1970. The authors wish to acknowledge the many stimulating discussions of this work that they enjoyed with their colleagues at the NASA Electronics Research Center. Particular credit is due to J. Canniff for programing the necessary computations.

* Staff Member, Man-Vehicle Laboratory. Member AIAA.
† Assistant Professor, College of Engineering. Member AIAA.
‡ Chief, Navigation and Guidance Branch.

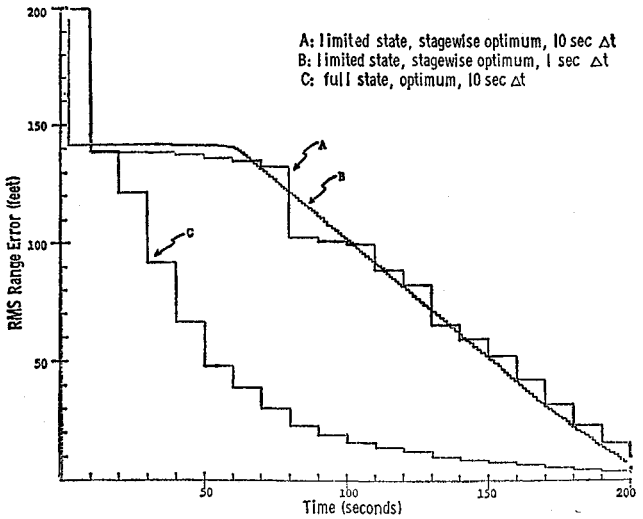

Fig. 1 Comparison of optimum and stagewise optimum filters.

additive measurement noise, are thus nonlinear, we shall suppose that the variations in range and scale factor from their nominal values are sufficiently small to justify a linearized analysis. In this case, the measurements z_i are

$$z_i = \rho_i + R + \rho_i S + v_i, \quad i = 1,2,\ldots \tag{1}$$

where ρ_i = nominal range at time of ith measurement; a linearly decreasing function of time, R = the variation in range (actual range minus nominal range); a constant because there is no variation in velocity, S = the variation in scale factor from a nominal value of unity; assumed constant, and v_i = additive measurement noise. Here ρ_i is a known function and R, S, v_1, v_2, ... are treated as uncorrelated random variables with zero mean values and known variances (σ_R^2, σ_S^2, and $\sigma_{v_i}^2 = \sigma_v^2$ for all i).

In order to make an optimal estimate of the range at each measurement time, it is necessary to construct a filter state x which summarizes all of the information obtained from the prior measurements. In the present case, the state would consist of two elements, which we can take to be the actual range and the scale factor error

$$x_i = \begin{bmatrix} \rho_i + R \\ S \end{bmatrix} \tag{2}$$

The optimum (in the sense of minimum mean squared error) linear estimator of x can then be written in the well known recursive form due to Kalman

$$\hat{x}_{i/i-1} = \hat{x}_{i-1/i-1} - \begin{bmatrix} V_0 \Delta t_i \\ 0 \end{bmatrix} \tag{3}$$

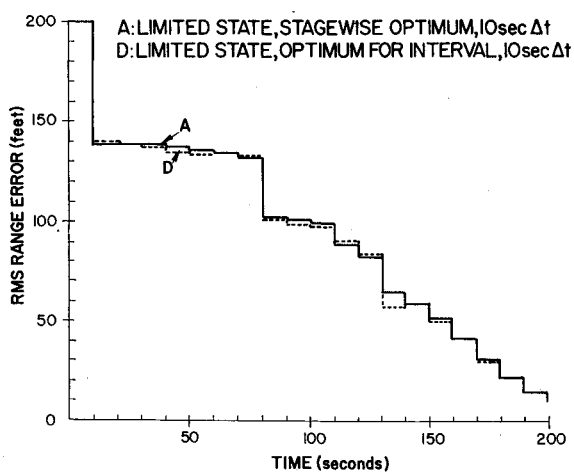

Fig. 2 Comparison of suboptimum point and interval estimators.

$$\hat{x}_{i/i} = \hat{x}_{i/i-1} + k_i(z_i - h_i^T x_{i/i-1}) \tag{4}$$

where $\hat{x}_{i/j}$ = best estimate of x_i based on all measurements taken up to time j ($z_1, z_2, \ldots, z_j$), $\hat{x}_{0/0} = \begin{bmatrix} \rho_0 \\ 0 \end{bmatrix}$ = best a priori estimate of x_0, V = known constant approach speed, Δt_i = time interval between ith and $(i-1)$th measurements, and $h_i^T = [1\ \rho_i]$ = measurement sensitivity to x_i and where the optimum two-dimensional gain k_i is related to the covariance matrix $P_{i/i-1}$ of the previous estimation error by

$$k_i = P_{i/i-1}h_i(h_i^T P_{i/i-1} h_i + \sigma_v^2)^{-1} \tag{5}$$

The covariance matrix is propagated and updated according to the equations

$$P_{i/i-1} = P_{i-1/i-1} \tag{6}$$

$$P_{i/i} = (I - k_i h_i^T)P_{i/i-1}(I - h_i k_i^T) + k_i \sigma_v^2 k_i^T \tag{7}$$

where

$P_{i/j} = \mathrm{cov}(1_{i/j})$

$1_{i/j} = \hat{x}_{i/j} - x_i$ = estimation error at time i with j measurements

$$P_{0/0} = \mathrm{cov}(1_{0/0}) = \mathrm{cov}(x_0) = \begin{bmatrix} \sigma_R^2 & 0 \\ 0 & \sigma_S^2 \end{bmatrix}$$

It is to be observed that the resulting filter produces optimum estimates of both the range and scale factor error at all times.

Motivated by this result, we now seek to reduce the storage requirements for the gains k_i by finding a recursive estimator for the range ($\rho + R \triangleq y$) in the form

$$\hat{y}_{i/i-1} = \hat{y}_{i-1/i-1} - \Delta V t_i \tag{8}$$

$$\hat{y}_{i/i} = \hat{y}_{i/i-1} + a_i(z_i - \hat{y}_{i/i-1}) \tag{9}$$

These equations correspond to Eqs. (3) and (4) with the constraint that k_i^T be of the form $[a_i, 0]$, in which case the scale factor error s is always estimated to be zero. The problem is to choose the scalar gains a_i in some best manner where we note that the variance equation (7) is valid for any choice of gain k_i.

III. Suboptimal Filters

One "best" method of computing the gains a_i when only range is to be estimated is to compute the optimum two-dimensional weighting vector k_i as previous [Eq. (5)] and then set the second element to zero. This choice of k_i must also be used to update P [Eq. (7)]. One can easily verify that this procedure produces a sequence of optimum single stage estimators in the sense that each a_i minimizes the resulting range

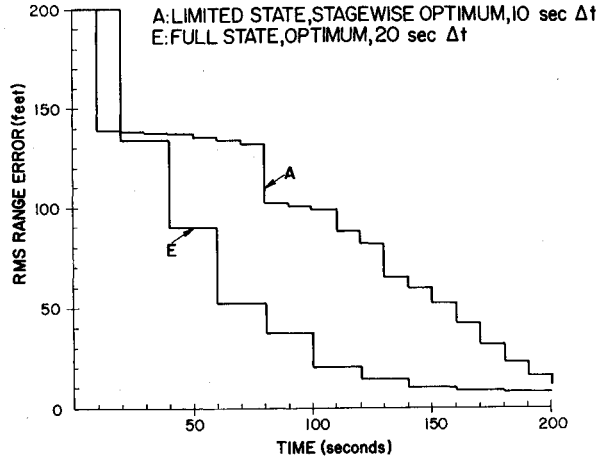

Fig. 3 Comparison of filters for fixed number of gains.

error variance at time i. But because y (in contrast to x) is not a sufficient statistic, one cannot expect that the estimate $y_{m/m}$ obtained after $m > 1$ measurements, will be the optimum combination of all these measurements.§ This fact is illustrated in Fig. 1 where the standard deviation in the range estimation error is plotted vs time for the optimal (2 state variable) filter and two stagewise optimal (range only) filters using different measurement intervals. The case considered was the following one

$$\text{initial covariance matrix} = \begin{bmatrix} (200)^2, & 0 \\ 0 & , \quad (0.01)^2 \end{bmatrix}$$

$$\text{initial range} = 20{,}000 \text{ ft}$$

$$\text{velocity} = 100 \text{ ft/sec}$$

$$\text{measurement noise variance} = (10 \text{ ft})^2$$

In addition to the fact that the stagewise optimum filters are clearly not optimum over-all, it will be observed that during some periods of time, better results (range only filters) are obtained with a 10 sec measurement interval than with a 1-sec interval. In other words, during these periods of time, the extra measurements actually result in worse performance!

As another criterion for choosing the gains a_i, we may seek to minimize the sum of the range error variances over the entire measurement schedule (a form of optimum interval estimation). Although this problem is simple to solve when the complete state is being estimated (the solution is the Kalman filter), an analytical solution for the limited state problem appears quite difficult to obtain. This optimal programming problem, of course, can be solved numerically; and the results obtained in this way are compared in Fig. 2 to the stagewise optimum results of Fig. 1 (10 sec measurement interval). It is noted that the performance of these two filters is not appreciably different for the particular problem considered here.

If we now consider the case in which only the terminal uncertainty is of interest, it is in fact possible to find a set of scalar gains a_i that will produce an over-all optimum estimate of the range at the terminal time. The reason for this is that, according to Eqs. (8) and (9), $y_{m/m}$ can be selected as an arbitrarily weighted combination of all the m measurements. The measurement weights, or equivalently, the gains a_i, thus can be chosen to produce the same terminal estimate of y as the optimum 2 state variable filter. Although this scheme could be implemented using the same recursive form as used for the previous schemes, it is important to realize that the intermediate values obtained are simply intermediate values in the estimation of the terminal range and are not useful estimates of the range at intermediate times. In fact, one can often do better by taking $y_{i/i} = y_{i/0} = \rho_i$.

Finally, we wish to point out that better results can be obtained for a fixed number of stored gains by reducing the number of measurements and estimating the complete state. This is illustrated in Fig. 3 where the performance of an optimum 2 state variable filter using 10 measurements, spaced 20 sec apart, is shown to be superior to that of the stagewise optimum range only filter using 20 measurements 10 sec apart (both cases requiring 20 stored gains.)

IV. Conclusions

In conclusion, it can be stated that the selection of a good limited state filter will require a careful statement of the constraints and measure of goodness to be employed. Further work is needed in this important area: to adequately explain some of the results reported here, to obtain possible analytical solutions, and to make a more general study of the penalties in performance that can result from using limited state recursive estimators.

§ The Kalman filter is sometimes "derived" as a superposition of single stage filters. This is valid only when the problem is formulated in the required Markov form.

Inclination of Pressure Orifices in Low-Density Flow

K. Kienappel*
Deutsche Forschungs- und Versuchsanstalt für Luft- und Raumfahrt, Aerodynamische Versuchsanstalt, Göttingen, Germany

1. Introduction

An important problem in rarefied gas dynamics is the interpretation given to the pressure measured in a cavity that is vented to the surface through an orifice. It has been found that the cavity pressure can differ markedly from the gas pressure when the temperatures of the cavity and the gas are different, and when the molecular mean free path is comparable to the orifice diameter. This is the so called "Orifice Effect." Previous investigators[1–5] have shown the dependence of this effect on orifice diameter and offer semi-empirical orifice-correction schemes that combine theoretical evaluation of the free molecule limit and correlated experimental data for the transitional flow regime. Recent experimental investigations[6] have shown a relationship between cavity pressure and orifice depth. For the first time the influence of the inclination angle of a pressure tube on the cavity pressure is shown in this Note.

2. Experiments

Experiments were performed with a cooled flat plate model in the hypersonic low-density wind tunnel of the DFVLR Göttingen.[7] The investigation was carried out at Mach numbers of 10 and 20. The freestream Reynolds numbers were in the range 300–1600/cm. The model has a row of nine pressure sampling points parallel to the leading edge. The outside holes, and the center one, were drilled perpendicular to the model surface. The others were inclined at angles between 30° and 80° relative to the leading edge.

3. Results

The static pressure distribution across the model was determined from measurements at the points where the holes are normal to the surface. This provides a reference pressure p_r for each sampling point. The measured pressure p_m normalized with the local reference pressure p_r is plotted in Fig. 1 vs the angle of inclination β. The experimental data show that p_m/p_r is a function of β and Reynolds number Re. The influence of β decreases with increasing Re.

In Fig. 2, p_m/p_r is plotted vs Re for a certain inclination angle β. The extrapolation through the set of the experi-

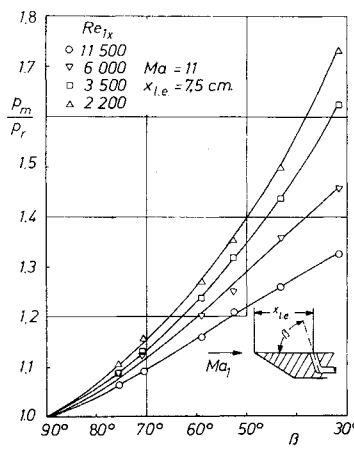

Fig. 1 Measured pressure p_m normalized with the local reference pressure P_r vs the angle of inclination β.

Received October 14, 1970; revision received December 17, 1970.

* Research Scientist.